# Organic & Biomolecular Chemistry

Accepted Manuscript






ROYAL SOCIETY OF CHEMISTRY

www.rsc.org/obc

# Photocontrol of Ion Permeation in Lipid Vesicles with Amphiphilic Dithienylethenes

Yamuna S. Kandasamy, Jianxin Cai, Alisha Beler, M.-S. Jemeli Sang, Patrick D. Andrews, R. Scott Murphy*

*Department of Chemistry and Biochemistry, University of Regina, 3737 Wascana Parkway, Regina, SK, S4S 0A2, Canada*

*scott.murphy.uregina@gmail.com*

## Abstract

The integration of photochromic dithienylethenes (DTEs) with lipid vesicles as photoresponsive membrane disruptors for ion transport applications has been examined. We have synthesized three amphiphilic DTEs **1**–**3** that incorporate a terminally charged alkyl chain, and contain methyl or phenylethynyl substituents at the reactive carbons. Our photochromic reactivity studies suggest that the inclusion of a single alkyl chain favors the photoactive antiparallel conformation of DTEs, given the significant improvement in the cyclization quantum yield over previous phenylethynyl derivatives. Our ion permeation studies show that the open-ring isomers of these DTEs are more disruptive than the closed-ring isomers in the four lipid vesicle systems studied, regardless of their lamellar phase at room temperature. In addition, a steric effect was clearly observed as DTEs incorporating the comparatively smaller methyl group exhibited lower rates of ion permeation than the bulkier phenylethynyl group. In all cases, UV irradiation led to a reduction in ion permeability. In fact, the methyl analog exhibited a significant reduction in ion permeability in gel-phase lipid vesicles upon UV exposure. Also, the hexyl chain derivatives had a greater effect on membrane permeability than the dodecyl derivative owing to their relative position in the bilayer membrane of lipid vesicles.

## Introduction

Biocompatible lipid-based nanoparticles (NPs) that perform photoinduced processes are continually being developed to improve function in applications such as drug delivery and ion transport.[1-7] These photoresponsive NPs allows for on-demand, pulsatile dosing from a single administration in biomedical applications. Further, light-triggered release provides a high level of spatiotemporal control. Thus far, photocontrols in lipid-based NPs has been primarily limited to irreversible processes, such as photocleavage and photopolymerization.[8-12] Reversible photocontrol of ion permeability in lipid vesicles has been reported for an amphiphilic azobenzene[13] and spiropyran[14]. In these studies, cycling between the isomeric states of the photochromic surfactants modulated ion permeabilities. The amphiphilic azobenzene was incorporated into anionic dihexadecylphosphate (DHP) vesicles. When these vesicles, loaded with potassium ions, were exposed to ultraviolet light, a *trans* to *cis* isomerization was observed but ion permeabilities only increased at temperatures approaching the phase transition temperature of DHP.[13] The amphiphilic spiropyran was also studied in DHP vesicles. Interestingly, a decrease in ion permeability was observed upon photoisomerization from the closed-ring spiro isomer to the open-ring merocyanine isomer. The leakage caused by the inclusion of the spiro form was interpreted as a disruption in the hydrocarbon chain packing, thus increasing the free volume within the membrane.[14] Whereas, isomerization to the merocyanine isomer resulted in its relocation to the polar head group region of the DHP vesicles, restoring membrane stability. However, both of these derivatives exhibit limited thermal stability. Dithienylethenes (DTEs) on the other hand are well known for their high thermal stability and high fatigue resistance allowing for repeated cycling between photoisomers.[15] To date, relatively few DTE amphiphiles have been synthesized.[16-20] For the majority of these DTEs, self-

assembled nanostructures were identified and reversible isomerization was observed in aqueous solution. Still, integrating amphiphilic DTEs with lipid vesicles to demonstrate photocontrol of ion permeability has not been reported. In a previous report, we examined a nonamphiphilic DTE containing methyl substituents at the reactive carbons.[21] Although photoisomerization of the DTE was reversible in lipid vesicles, the release of an encapsulated fluorophore was not observed upon cycling between isomeric states. It was proposed that disruption within the bilayer membrane was insufficient for the permeation of a hydrophilic dye molecule. Consequently, the goals of this paper are to report on the synthesis of three new amphiphilic DTEs (Chart 1), two of which integrate bulkier phenylethynyl substituents that undergo larger changes in molecular geometry upon photoisomerization[22, 23], to characterize their photochromic reactivity, to integrate them into four lipid systems of varying lamellar phase, and to examine their photocontrol of ion permeability through a bilayer membrane using a ratiometric fluorescence assay. <Chart 1>

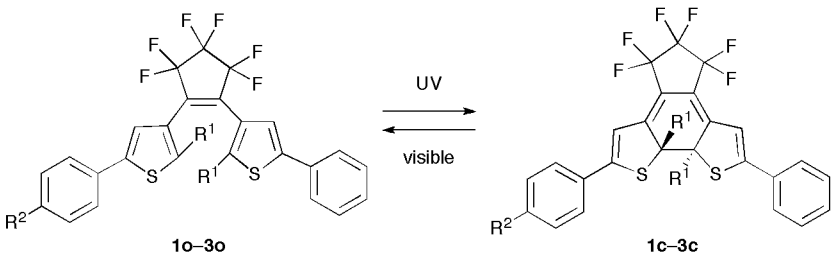


**Chart 1.** Structures of the dithienylethene photoisomers for **1**–**3**.

## Results and discussion

**Synthesis of asymmetrical amphiphilic DTEs.** We have synthesized asymmetrical DTEs **1** and **2** that contain rigid phenylethynyl substituents at the reactive carbons, which participate in the electrocyclic ring-closing and ring-opening reactions. These substituents were chosen for their increased steric bulk compared with DTE **3** that contains methyl groups at the reactive carbons. Further, we have enhanced the lipid complementarity of these DTEs by incorporating cationic alkyl ammonium substituents.

We have previously shown that the presence of potentially reactive alkyne substituents does present some limitations to the relative substitution order on thiophene.[23] For this reason, we used a regioselective approach that introduces functional groups at periphery of the thiophene prior to the introduction of the alkynyl substituents. The inclusion of a cationic alkyl ammonium substituent into asymmetrical DTEs **1**–**3** begins with amino acids as starting materials. Our synthetic methodology started with the conversion of amino acids to tertiary alkyl amines. There are several reported methods for the conversion of primary amines to tertiary amines.[24] One such method involves the direct alkylation of a primary amine by an alkyl halide. However, this approach is rarely used because the degree of alkylation is difficult to control. Alternatively, reductive amination can be used to overcome this obstacle. Initially, we carried out this reaction with formaldehyde using a Zn/acetic acid condition as a hydrogen source instead of hydrogen gas/palladium on carbon. The former reaction works well, but requires a longer reaction time (i.e., > 24 h) to complete the alkylation than the latter. As a result, we chose successive alkylation of a primary amine via a secondary amine to tertiary alkyl amine in one pot in the presence of hydrogen gas/palladium on carbon.[25] The carboxylic acids were then reacted with thionyl chloride to produce acyl chlorides[26], which were used in the Friedel-Crafts acylation of

bromobenzene[27] to produce **4** and **5** in moderate yields (Scheme 1). Wolff-Kishner reduction of these ketones at high temperature produced **6** and **7** as pale yellow oils. These compounds were then converted to the corresponding boronic acids, which were used in Suzuki reactions without further purification. Using crude boronic acids in the coupling reactions with 2,4-dibromothiophene did not significantly affect the yields of **8** and **9**. The electrophilic bromination of the coupled products was achieved in good yield to produce **10** and **11** using *N*-bromosuccinimide (NBS) as the brominating reagent in an acetic anhydride/acetic acid solution.[28] Initially, we had used NBS and 10 mol% perchloric acid as a phase-transfer catalyst.[29] However, reaction times were significantly longer (i.e., greater than three fold) under these reaction conditions. Notably, bromination of the *p*-phenylene unit was not observed. The phenylethynyl substituent was introduced using a Sonogashira reaction by coupling ethynylbenzene to the bromo-substituted products to give **12** and **13** in good yield. The final coupling of **12** and **13** with **14**, which itself was synthesized by the coupling of a phenyl derivative with excess octafluorocyclopentene, gave neutral DTEs **15** and **16** in moderate yields. The final asymmetrical DTEs **1** and **2** were formed by methylation of the tertiary alkylamine side chains using iodomethane. DTE **3** was prepared like **2** except 3,5-dibromo-2-methylthiophene was used to introduce methyl substituents at the reactive carbons (Scheme 2).

<Schemes 1 and 2>

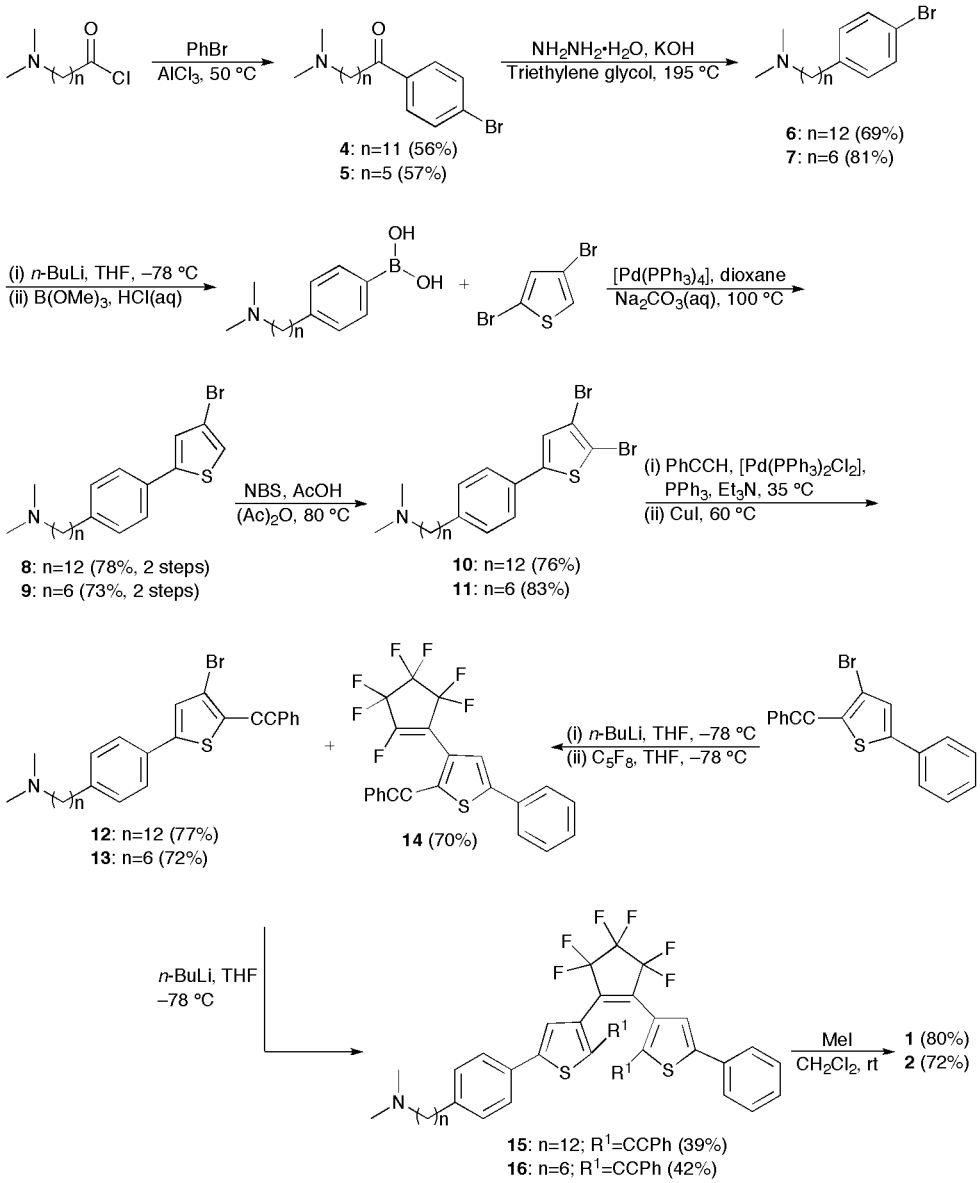


**Scheme 1.** Synthesis of **1** and **2**.

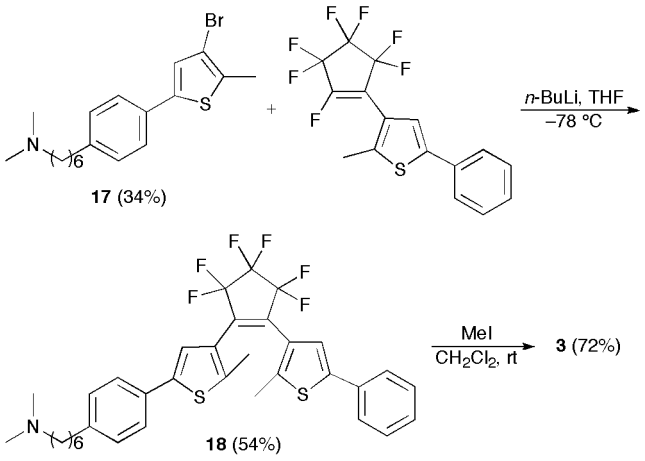


**Scheme 2.** Synthesis of **3**.

**Quantum yields, photoconversions, and fatigue resistance.** Compounds **1**–**3** were observed to undergo reversible photoisomerization in ethyl acetate. Upon irradiation with UV light, a pale yellow solution of **1o** turned blue and an increase in absorbance was observed at 585 nm with a concomitant decrease at 310 nm (Figure 1). This new absorption band in the visible region represents the formation of the closed-ring isomer **1c**. The wavelengths of maximum absorption ($\lambda_{max}$) for **1** and **2** were similar to other DTEs with phenylethynyl substituents at the reactive carbons.[23] Further irradiation of **1** with UV light brought the system to a photostationary state of the open-ring and closed-ring isomers. Notably, the photoconversion for asymmetrical DTE **1o** integrating a terminally charged dodecyl chain was two fold larger than a symmetrical DTE with uncharged dodecyl chains we previously reported (i.e., 21 ± 2%).[23] The conversion efficiency for **3o** was moderately higher with respect to **1** and **2**. This agrees well with alkyl-substituted DTEs with methyl substituents at the reactive carbons.[30] The photoisomerization of **1c**–**3c** were completely reversible following irradiation with visible light. In addition, no thermal discoloration of **1c**–**3c** was observed after 24 h in the dark at room temperature. <Figure 1 and Table 1>

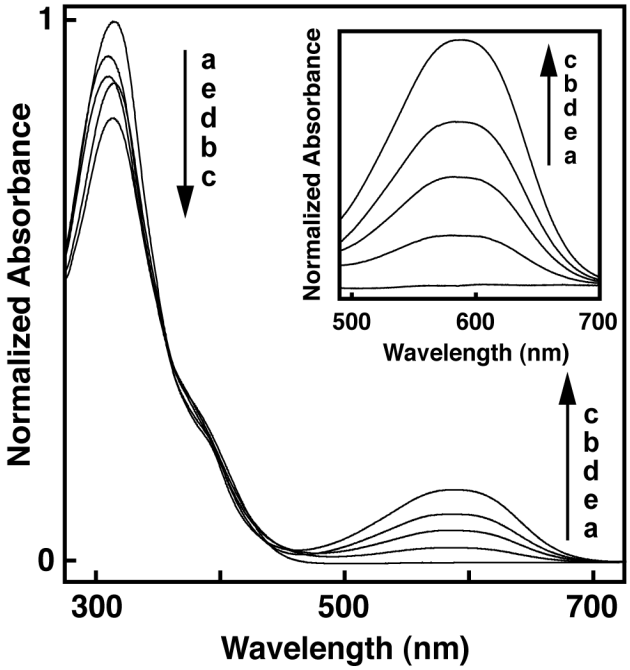


**Fig. 1.** Normalized absorption spectra of **1** in ethyl acetate prior to irradiation (a) and after irradiation with UV or visible light in the following sequence: (b) 1 min of UV, (c) 3 min of UV, (d) 15 s of visible, and (e) 30 s of visible. The inset is an expansion of the 490–700 nm region.

**Table 1.** Absorption Properties and Photochromic Reactivity of Dithienylethenes (DTE) in Ethyl Acetate[a]

| DTE | $\lambda_{max}$ (nm)[b] | $\varepsilon_{max}$ ($10^4$ $M^{-1}$ $cm^{-1}$) | $\phi_{o\rightarrow c}$[c] | DTE | $\lambda_{max}$ (nm)[b] | $\varepsilon_{max}$ ($10^3$ $M^{-1}$ $cm^{-1}$) | $\phi_{c\rightarrow o}$[d] | Conversion (%) |
|---|---|---|---|---|---|---|---|---|
| **1o** | 310 | 1.93 ± 0.09 | 0.28 ± 0.03 | **1c** | 585 | 4.72 ± 0.05 | 0.38 ± 0.08 | 51.7 ± 0.4 |
| **2o** | 312 | 4.17 ± 0.50 | 0.10 ± 0.02 | **2c** | 585 | 9.80 ± 0.82 | 0.15 ± 0.01 | 48.1 ± 0.5 |
| **3o** | 288 | 3.85 ± 0.18 | 0.46 ± 0.02 | **3c** | 588 | 16.40 ± 0.43 | 0.008 ± 0.001 | 81.8 ± 0.3 |

[a] The error is the standard deviation for the mean taken from a minimum of three independent measurements.
[b] The error is ± 1 nm.
[c] Cyclization quantum yield.
[d] Cycloreversion quantum yield.

The cyclization and cycloreversion quantum yields of **1**–**3** were also determined in ethyl acetate. An equilibrium mixture of two conformers (i.e., parallel and antiparallel) exists for DTEs in solution. The conrotatory photocyclization reaction can proceed only from the antiparallel conformation.[15] Consequently, the cyclization quantum yield is dependent on the ratio of the conformations. When the ratio of the photoactive antiparallel conformation is increased, the quantum yield is expected to increase. The cyclization quantum yield for **1o** was two fold higher than the parent phenylethynyl derivative without alkyl chain substituents (i.e., $\phi_{o\rightarrow c} = 0.14 \pm 0.01$[23]) and eight fold higher than a symmetrical DTE with dodecyl chains (i.e., $\phi_{o\rightarrow c} = 0.036 \pm 0.002$[23]). For the latter, we hypothesized that intramolecular interactions between dodecyl chains would favor the photoinert parallel conformation, thus lowering the cyclization quantum yield. Our results suggest that the inclusion of a single alkyl chain favors the photoactive conformation. Consequently, the asymmetrical nature of **1** is a significant improvement over the former symmetrical dodecyl derivative and the parent phenylethynyl system. The cyclization quantum yield of **2o** was also higher (i.e., ca. three fold) than the symmetrical dodecyl derivative but similar to the parent system. It is apparent that the length of the alkyl chain plays a role but the exact nature of this effect on the cyclization quantum yield will require further study. A similar correlation is observed for the cycloreversion quantum yields. In general, the introduction of phenylethynyl substituents at the reactive carbons of DTEs has been shown to enhance the efficiency of the cycloreversion reaction relative to the cyclization reaction.[22, 23] We observed similar enhancements for **1c** and **2c**. Notably, the cycloreversion quantum yield for **2c** was 18-fold larger than its methyl analog **3c**. In addition, the cycloreversion quantum yield for **1c** was three fold higher than the symmetrical dodecyl derivative (i.e., $\phi_{c\rightarrow o} = 0.13 \pm 0.01$[23]) and similar to the parent phenylethynyl derivative without

alkyl substitution (i.e., $\phi_{c\rightarrow o} = 0.44 \pm 0.02$[23]). This suggests that the inclusion of phenylethynyl substituents has a much larger effect on the cycloreversion quantum yield than the integration of a single alkyl chain.

The photostability of **1**–**3** was measured by UV-vis absorption spectroscopy over five ring-closing/ring-opening cycles in ethyl acetate in the presence of air (Figure S1, Electronic Supplementary Information (ESI)). For each DTE, the absorbance was monitored at the $\lambda_{max}$ of the ring-closed isomer. Overall, the fatigue resistance of these DTEs was found to increase in the order of **1** < **2** < **3**, with 17%, 14%, and 5% degradation, respectively. These results suggest that the presence of phenylethynyl substituents in DTEs (i.e., **1** and **2**) decreases their photostability relative to the presence of a methyl group, as in **3**. This irreversible photodegradation is consistent with previous reports[23] and results from UV irradiation of the closed-ring isomers to isomeric photostable byproducts (Chart S1, ESI). For example, the prolonged UV irradiation of **1o** beyond the photostationary state resulted in two new resonances at 6.68 and 6.83 ppm in the $^1$H NMR spectrum (Figure S2, ESI). The resonance at 6.83 ppm is assigned to the closed-ring isomer (**1c**) and the resonance at 6.67 ppm to the photostable byproduct (**1b**). Further, the signal at 6.83 ppm of **1c** decreases with the concomitant growth of the **1b** signal at 6.67 ppm. This suggests that **1b** is a product of the photolysis of the precursor **1c** as reported by others[31-34]. Further, the formation of photostable byproducts in DTEs has been proposed to involve a methylcyclopentene diradical as a possible intermediate.[35, 36] If true, this would explain the decreased photostability observed for the phenylethynyl derivatives **1** and **2** relative to the methyl derivative **3**, as the alkynyl substituent would stabilize the diradical intermediate via resonance.

**Ion permeation studies in lipid vesicles.** The photocontrol of ion permeability for lipid vesicles incorporating DTEs **1**–**3** was assessed using a common ratiometric fluorescence technique[37, 38] in which these vesicles are encapsulated with a pH-sensitive fluorophore, 8-hydroxypyrene-1,3,6-trisulfonic acid (HPTS), during their preparation. The fluorescence of these vesicles is stable prior to the injection of a base pulse, which creates a transmembrane pH gradient. This gradient will collapse if there is an increase in membrane permeability due to the presence of DTE in either isomeric state. The emission maximum for HPTS is the same for both the acid and conjugate base forms; however, the excitation wavelengths differ. As a result, the acid/base ratio can be determined from the emission intensity modulation produced by alternating the excitation wavelength. This modulated emission signal can be converted to a normalized fraction of ion permeation for which the rate of ion permeation can be determined using a procedure described previously (Figure 2).[37] This assay was performed in the dark to assess vesicle stability and with UV irradiation to determine the effect of DTE isomerization on ion permeability. Given the batch-to-batch variability commonly observed with lipid vesicle studies[37], vesicles incorporating DTEs were compared with control vesicles composed of only lipids. These comparisons help to ensure that the changes observed are due to the effect that DTEs as either the open-ring or closed-ring isomers have on the permeability of the lipid vesicles. <Figure 2>

We have examined DTEs in four different lipid systems, namely 1,2-dipalmitoyl-*sn*-glycero-3-phosphocholine (DPPC), 1,2-dioleoyl-*sn*-glycero-3-phosphocholine (DOPC), 1,2-diphytanoyl-*sn*-glycero-3-phosphocholine (diPhyPC), and lecithin. The phase state of these lipid systems is dependent on temperature. At room temperature, DPPC vesicles are in the gel phase, whereas DOPC, diPhyPC, and lecithin vesicles are in the fluid phase.[39] The lipid diPhyPC was chosen given this lipid has no detectable gel to liquid crystalline phase transition from –120 to 80

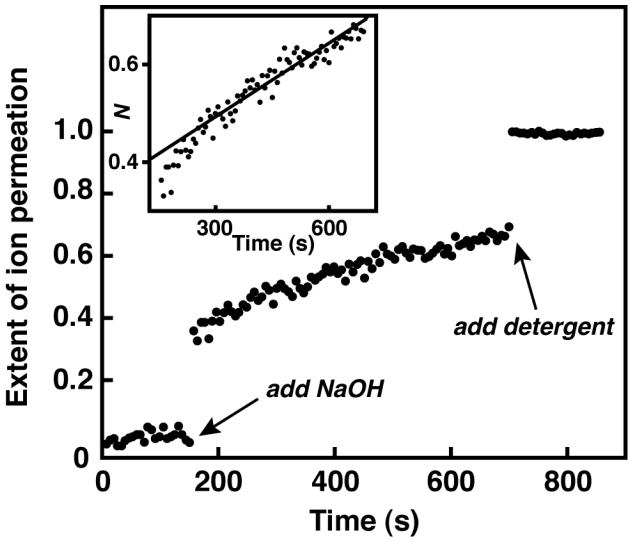


**Fig. 2.** Extent of ion permeation as a function of time for **2** in DPPC vesicles. The inset is a linear fit to data > 180 s.

°C due to its branched acyl chains.[40] In addition, lecithin was used to represent a mixture of saturated and unsaturated PC lipids predominantly composed of unsaturated acyl chains (e.g., linoleyl and oleyl). Before incorporating our photochromic compounds into lipid vesicles, the rates of ion permeation for control vesicles with and without UV irradiation were compared. The rate constants increased in the following order: DPPC < DOPC ≈ diPhyPC < lecithin (Table 2). Consistent with earlier studies,[41] this trend suggests that DPPC in its gel phase is less permeable to ions than the other lipids in their fluid phase by at least a factor of four and greater than six fold when compared to lecithin prior to irradiation. A slight decrease in rates was observed for all control lipid vesicles following irradiation, although within error of the rates observed before irradiation. In general, the pore mechanism has been used to describe proton permeation in bilayer membranes composed of pure lipids with chain lengths less than 20 carbons.[42] This mechanism proposes that permeation across a bilayer membrane occurs through transient hydrated pores produced by thermal fluctuations. Permeation via these hydrated defects allows protons to avoid

the high-energy barrier associated with partitioning into the hydrophobic membrane interior, which is commonly described as the solubility–diffusion mechanism. This alternative mechanism is often used to describe the permeation of larger ions (e.g., potassium) and neutral molecules in lipid vesicles[42], including those incorporating photochromic amphiphiles.[13, 14, 43] The stability of the lipid systems can also be interpreted from the extent of ion permeation. Similar to the rate constant comparisons, DPPC control vesicles were found to be more stable than lipid vesicles in the fluid phase (Table 3). A slight increase in the extent of ion permeation was observed for all the fluid-phase control vesicles following irradiation, although within error of those observed before irradiation. Further, a relatively larger change was observed for the gel-phase, DPPC control vesicles following irradiation. We partly attribute the magnitude of this change to the higher stability of the nonirradiated DPPC vesicles, which are ca. five fold less permeable than the fluid-phase vesicles. As a result, the observed increase for DPPC vesicles following irradiation appears somewhat amplified when compared with the fluid-phase control vesicles. In fact, the extent of ion permeation for the irradiated DPPC control vesicles is still lower than all the irradiated fluid-phase control vesicles. The leakage observed in these control samples is primarily due to the transmembrane pH gradient created by the pH pulse and the subsequent pH equilibration as vesicles adjust to ionic and osmotic stresses via transient pore formation within the bilayer.[44] In this way, the HPTS assay will be used to probe the formation of additional pores or defects in bilayer membranes resulting from the incorporation and isomerization of amphiphilic DTEs.
<Tables 2 and 3>

The rate constants of ion permeation and the extent of ion permeation were initially examined for **1** and **2** to assess the effect of the alkyl chain length on membrane permeability. In

addition, these values were compared with control vesicles and presented as ratios. Prior to UV irradiation, the permeation rate constants for **1** and **2** in DPPC vesicles at a mole ratio of 1:20

**Table 2.** Ion permeation rate constants determined in various lipid vesicles at a mole ratio of 1:20 DTE/lipid[a]

| Lipid | DPPC | | | | Lecithin | | | |
|---|---|---|---|---|---|---|---|---|
| | k ($10^{-4}$ $s^{-1}$) | | Ratio[b] | | k ($10^{-4}$ $s^{-1}$) | | Ratio[b] | |
| UV | No | Yes | No | Yes | No | Yes | No | Yes |
| Control | 0.46 ± 0.26 | 0.31 ± 0.28 | 1 | 1 | 3.1 ± 1.0 | 2.6 ± 1.0 | 1 | 1 |
| **1** | 4.2 ± 1.4 | 2.3 ± 1.1 | 9.1 | 7.4 | 6.6 ± 1.2 | 3.3 ± 1.4 | 2.1 | 1.3 |
| **2** | 4.8 ± 1.0 | 1.6 ± 0.5 | 10.4 | 5.2 | 4.9 ± 0.6 | 3.3 ± 0.5 | 1.6 | 1.3 |
| **3** | 2.6 ± 0.4 | 0.20 ± 0.16 | 5.7 | 0.65 | 4.5 ± 0.4 | 3.2 ± 0.2 | 1.5 | 1.2 |
| **15** | 4.4 ± 0.4 | 2.2 ± 0.4 | 9.6 | 7.1 | 1.3 ± 0.2[c] | 0.18 ± 0.01[c] | 0.42 | 0.07 |
| **16** | 3.9 ± 0.3 | 1.8 ± 0.4 | 8.5 | 5.8 | 1.5 ± 0.2[c] | 0.60 ± 0.11[c] | 0.48 | 0.23 |
| Lipid | DOPC | | | | diPhyPC | | | |
| | k ($10^{-4}$ $s^{-1}$) | | Ratio[b] | | k ($10^{-4}$ $s^{-1}$) | | Ratio[b] | |
| UV | No | Yes | No | Yes | No | Yes | No | Yes |
| Control | 1.9 ± 0.4 | 1.5 ± 0.3 | 1 | 1 | 1.8 ± 0.4 | 1.3 ± 0.4 | 1 | 1 |
| **1** | 3.0 ± 0.6 | 2.3 ± 0.5 | 1.6 | 1.5 | 3.9 ± 0.5 | 2.3 ± 0.6 | 2.2 | 1.8 |
| **2** | 3.2 ± 0.3 | 1.5 ± 0.5 | 1.7 | 1.0 | 3.7 ± 0.5 | 1.8 ± 0.4 | 2.1 | 1.4 |
| **3** | 1.7 ± 0.1 | 0.76 ± 0.14 | 0.89 | 0.51 | 2.4 ± 0.7 | 0.47 ± 0.14 | 1.3 | 0.36 |
| **15** | 5.4 ± 0.3[c] | 4.5 ± 0.1[c] | 2.8 | 3.0 | 4.4 ± 0.2 | 2.4 ± 0.2 | 2.4 | 1.8 |
| **16** | 6.6 ± 0.3[c] | 5.5 ± 0.4[c] | 3.5 | 3.7 | 3.4 ± 0.2 | 1.7 ± 0.3 | 1.9 | 1.3 |

[a] The error is the standard deviation for the mean taken from a minimum of three independent measurements.
[b] Represents the ratio of the rate constants of ion permeation for the sample versus the control.
[c] A mole ratio of 1:30 DTE/lipid was used.

**Table 3.** Normalized extent of ion permeation determined in various lipid vesicles at a mole ratio of 1:20 DTE/lipid[a]

| Lipid | DPPC | | | | Lecithin | | | |
|---|---|---|---|---|---|---|---|---|
| | *N* | | Ratio[b] | | *N* | | Ratio[b] | |
| UV | No | Yes | No | Yes | No | Yes | No | Yes |
| Control | 0.07 ± 0.06 | 0.22 ± 0.07 | 1 | 1 | 0.39 ± 0.12 | 0.45 ± 0.13 | 1 | 1 |
| **1** | 0.54 ± 0.08 | 0.56 ± 0.11 | 7.7 | 2.5 | 0.68 ± 0.10 | 0.66 ± 0.10 | 1.7 | 1.5 |
| **2** | 0.69 ± 0.04 | 0.59 ± 0.07 | 9.9 | 2.7 | 0.58 ± 0.12 | 0.55 ± 0.14 | 1.5 | 1.2 |
| **3** | 0.67 ± 0.07 | 0.43 ± 0.07 | 9.6 | 2.0 | 0.42 ± 0.01 | 0.50 ± 0.03 | 1.1 | 1.1 |
| **15** | 0.56 ± 0.07 | 0.53 ± 0.04 | 8.0 | 2.4 | 0.54 ± 0.03[c] | 0.50 ± 0.06[c] | 1.4 | 1.1 |
| **16** | 0.56 ± 0.07 | 0.51 ± 0.13 | 8.0 | 2.3 | 0.90 ± 0.01[c] | 0.83 ± 0.02[c] | 2.3 | 1.8 |
| Lipid | DOPC | | | | diPhyPC | | | |
| | *N* | | Ratio[b] | | *N* | | Ratio[b] | |
| UV | No | Yes | No | Yes | No | Yes | No | Yes |
| Control | 0.33 ± 0.08 | 0.37 ± 0.07 | 1 | 1 | 0.35 ± 0.08 | 0.45 ± 0.09 | 1 | 1 |
| **1** | 0.60 ± 0.02 | 0.66 ± 0.04 | 1.8 | 1.8 | 0.54 ± 0.07 | 0.56 ± 0.04 | 1.5 | 1.2 |
| **2** | 0.69 ± 0.09 | 0.69 ± 0.09 | 2.1 | 1.9 | 0.66 ± 0.05 | 0.64 ± 0.07 | 1.9 | 1.4 |
| **3** | 0.23 ± 0.06 | 0.23 ± 0.02 | 0.70 | 0.62 | 0.49 ± 0.07 | 0.31 ± 0.05 | 1.4 | 0.69 |
| **15** | 0.90 ± 0.02[c] | 0.81 ± 0.03[c] | 2.7 | 2.2 | 0.89 ± 0.01 | 0.71 ± 0.04 | 2.5 | 1.6 |
| **16** | 0.94 ± 0.02[c] | 0.89 ± 0.02[c] | 2.8 | 2.4 | 0.79 ± 0.02 | 0.62 ± 0.05 | 2.3 | 1.4 |

[a] The error is the standard deviation for the mean taken from a minimum of three independent measurements.
[b] Represents the ratio of the extents of ion permeation for the sample versus the control.
[c] A mole ratio of 1:30 DTE/lipid was used.

DTE/DPPC were at least nine fold higher than the control vesicles following the addition of the base pulse (Table 2). The inclusion of DTEs most likely disrupts bilayer packing, promoting the formation of bilayer defects within the membrane. Following irradiation a two fold decrease was observed for **2** and only a minor decrease was observed for **1**. Further, the ratios representing the extent of ion permeation decreased by at least three fold for both **1** and **2** upon photoisomerization to the closed-ring isomers (Table 3). These results suggest that the open-ring isomers of **1** and **2** are more disruptive than the closed-ring isomers in DPPC vesicles. Although the molecular volume of the closed-ring isomers is larger[22], the increased conformational mobility associated with the open-ring isomers and its organization within the membrane may promote the formation of a greater number of bilayer defects. While the rate constant or extent of permeation for these systems are not lowered to control values following irradiation, they do exhibit a moderate level of photocontrol. Moreover, the alkyl chain length appears to have an effect as well due to the relative positioning of the photochromic moiety in the lipid bilayer. For example, the shorter hexyl derivative has a greater effect on the extent of ion permeation given the closer proximity of the photochromic moiety to the phospholipid head group region of the lipid bilayer. Previously, spirooxazines with varying alkyl chain lengths were examined in DPPC vesicles to assess the free volume distribution in a bilayer membrane.[45] The smallest free volume was found in the phospholipid head group region, while the largest free volume was detected in the interior aliphatic region. It is reasonable to assume that the photochromic moiety would be more easily accommodated in regions of increased free volume. Consistent with this view, the inclusion of **2** appears to have a greater effect on membrane permeability than **1**.

Unlike DPPC vesicles, relative changes in the extent of ion permeation for diPhyPC, DOPC, and lecithin vesicles incorporating **1** and **2** were similar. In all cases, a decrease in the ratios was observed following UV irradiation, which again suggests a slight preference for the closed-ring isomer. However, the differences were much smaller than in DPPC. This was anticipated given lipids in their fluid phase are more flexible and permit rapid reorganization when compared to gel-phase lipids.[41, 43] In DOPC and diPhyPC vesicles, a >30% decrease in the ratio of rate constants for **2** following UV irradiation was observed, whereas the decrease in the presence of **1** was less significant. Similar to our observations in DPPC, **2** may be a more effective membrane disruptor in these lipid systems due to its relative position in the bilayer. In lecithin, **1** appeared to be more effective with a similar 30% decrease, although the errors were significantly larger. In contrast to DPPC, the rates of permeation observed for the fluid-phase lipids following UV exposure are significantly closer to control levels. This would indicate that the presence of the closed-ring isomers of **1** and **2** in fluid-phase lipid vesicles has a minor effect on rate of ion permeation.

To evaluate the effect of the phenylethynyl substituent on membrane permeability, we examined **3**, an analog of **2** that has methyl substituents at the reactive carbons. At a mole ratio of 1:20, we observed the lowest rate constants compared with all the DTEs in all lipid systems. Notably, upon UV irradiation of **3** in DPPC the ratio of rate constants decreased nine fold to control levels. A reduction in the ratio of rate constants was also observed in DOPC and diPhyPC, whereas for lecithin the change was small and similar to **2**. Interestingly, for DOPC and diPhyPC the rate constants were near control levels before UV irradiation and reduced to below control levels after irradiation, suggesting the closed-ring isomer of **3** stabilizes these vesicles. For the majority of cases there is a clear steric effect. The comparatively smaller

methyl substituent exhibits lower rates of ion permeation than the bulkier phenylethynyl substituent as open-ring isomers. Comparing the relative extents of ion permeation, the methyl derivative **3** is generally less disruptive than the analogous phenylethynyl derivative **2**. Further, lipid vesicles in the fluid phase were less permeable in the presence of **3** than with **2**. In particular, DOPC vesicles were three fold less permeable. Upon UV irradiation of **3** in DPPC vesicles, we observed a five fold decrease in membrane permeability. Again, these results indicate that the open-ring isomers are more disruptive than the closed-ring isomers. Overall, these results suggest that **3** provides better photocontrol of proton permeability in bilayer membranes, given the photoinduced changes are larger than **2** and the vesicles are generally more stable before and after irradiation.

Given the largest photoinduced changes were observed in DPPC, we studied **1**–**3** in DPPC vesicles at various mole ratios to examine the effect of their concentration on vesicle permeability. In general, we think of our DTEs as membrane disruptors rather than membrane transporters. Nevertheless, by monitoring the extent of ion permeation as a function of DTE concentration, we can determine Hill coefficients (*n*) to qualitatively assess aggregation behavior.[38] For **1o**–**3o** in DPPC vesicles, *n* values were ca. 1 which suggests that the active structure is a DTE monomer (Table S1, ESI).[46] Following UV irradiation, *n* values for **1c**–**3c** in DPPC vesicles were within error of the coefficients observed before irradiation. As a result, DTE aggregation within the membrane is not significant and not a rate-determining condition of ion permeation. Yet, as expected, varying the concentration of **1**–**3** in DPPC vesicles did affect both the rate and extent of ion permeation. Increasing the mole ratio of **3** from 1:20 to 1:10 **3**/DPPC resulted in the disruption of lipid vesicles following the addition of base as clearly seen from the extent of ion permeation prior to irradiation (Figure 3 and Table 4). Decreasing the

mole ratio to 1:40 significantly lowered ion leakage five fold, although these vesicles were still three fold more permeable than the control. Still, the largest photoinduced changes were observed at a mole ratio of 1:20. Similar to **3**, vesicle stability is compromised prior to UV irradiation and after the base pulse when **2** was included at a mole ratio of 1:10 (Figure S3 and Table S2, ESI). Interestingly, DPPC vesicles incorporating **1** were not compromised at the same mole ratio, although they were very permeable (Figure S4 and Table S3, ESI). Again, this difference in permeability suggests that the hexyl derivatives **2** and **3** do have a greater effect on vesicle stability compared with the dodecyl derivative **1** owing to their closer proximity to the head group region of the lipid bilayer. UV irradiation of **1** and **2** in DPPC did result in a ca. three fold reduction in the extent of ion permeation at all mole ratios, with the exception of **2** at 1:20 which is ca. four fold lower. The rate constants for ion permeation also decreased ca. 2-3 fold upon formation of the closed-ring isomers of **1** and **2**. Further, these changes were greater for **2** when compared with **1** at all mole ratios but still lower than that observed for **3**. Again, these results show that chain length and substitution have a large effect on vesicle stability. Moreover, the concentration of photochromic compound also has a significant effect on the stability of the host vesicle and the overall photocontrol of ion permeability in DPPC vesicles. <Figure 3 and Table 4>

To evaluate the effect of the amphiphilic structure of **1** and **2** on membrane permeability, we also examined the neutral precursors **15** and **16** in lipid vesicles. The cationic quaternary ammonium substituent terminally tethered to the alkyl chains of **1** and **2** represents a simplified mimic of the polar choline head group in phospholipids. Thus, it was hypothesized that DTEs integrating a cationic substituent would be better organized within the bilayer of phosphatidylcholine vesicles, whereas DTEs with neutral substituents would be less organized

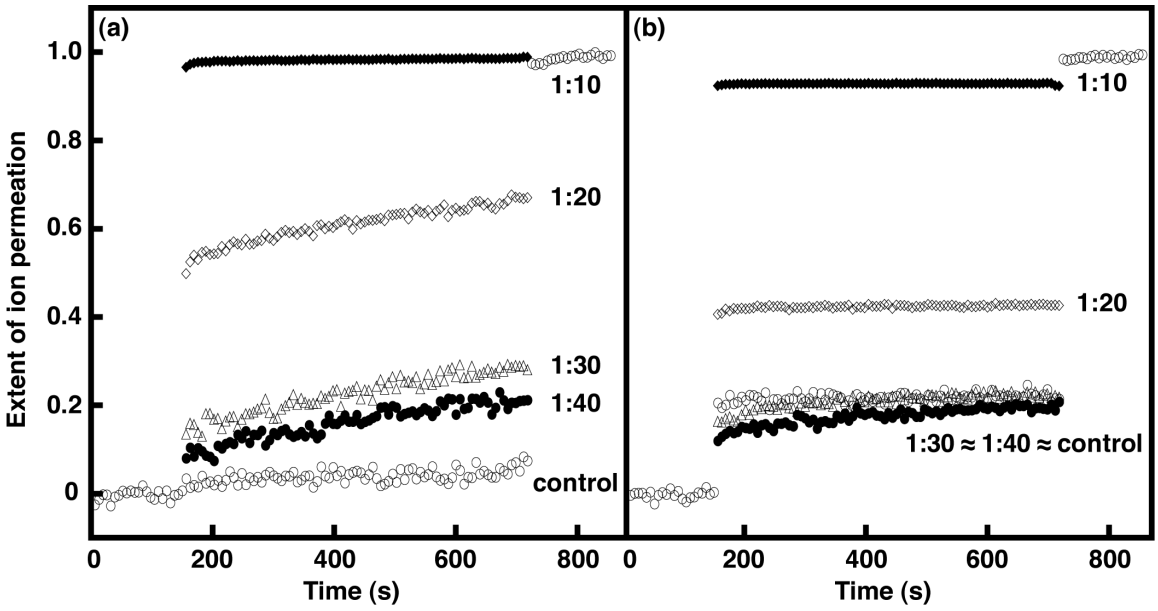


**Fig. 3.** Extent of ion permeation as a function of time for various mole ratios of **3** in DPPC vesicles (i.e., **3**/DPPC) prior to UV irradiation (a) and after 3 min of UV irradiation (b). For clarity only the control is shown before the base pulse and after the addition of detergent.

**Table 4.** Ion permeation rate constants and normalized extent of ion permeation determined for **3** in DPPC vesicles at various mole ratios[a]

| **3**/DPPC | k ($10^{-4}$ $s^{-1}$) | | Ratio[b] | | *N* | | Ratio[c] | |
|---|---|---|---|---|---|---|---|---|
| UV | No | Yes | No | Yes | No | Yes | No | Yes |
| Control | 0.46 ± 0.26 | 0.31 ± 0.28 | 1 | 1 | 0.07 ± 0.06 | 0.22 ± 0.07 | 1 | 1 |
| 1:10 | 0.17 ± 0.01 | 0.03 ± 0.01 | 0.37 | 0.10 | 0.99 ± 0.01 | 0.93 ± 0.02 | 14.1 | 4.2 |
| 1:20 | 2.6 ± 0.4 | 0.20 ± 0.16 | 5.7 | 0.65 | 0.67 ± 0.07 | 0.43 ± 0.07 | 9.6 | 2.0 |
| 1:30 | 2.5 ± 0.4 | 0.78 ± 0.42 | 5.4 | 2.5 | 0.29 ± 0.08 | 0.22 ± 0.14 | 4.1 | 1.0 |
| 1:40 | 2.3 ± 0.5 | 0.56 ± 0.41 | 5.0 | 1.8 | 0.21 ± 0.05 | 0.20 ± 0.14 | 3.0 | 0.91 |

[a] The error is the standard deviation for the mean taken from a minimum of three independent measurements.
[b] Represents the ratio of the rate constants of ion permeation for the sample versus the control.
[c] Represents the ratio of the extents of ion permeation for the sample versus the control.

and primarily reside in the hydrophobic aliphatic region of the lipid bilayer. However, the tertiary amino substituents of **15** and **16** are ionizable and presumably protonated in the presence of phosphate buffer given the $pK_a$ for a similar tertiary amine is ca. 9.8. Nonetheless, we did observe a significant effect on ion permeability in fluid-phase lipid vesicles, particularly in DOPC and lecithin. At a mole ratio of 1:20, these vesicles were not stable after the addition of base as the extent of ion permeation was essentially unity. As a result, we examined **15** and **16** at a lower mole ratio of 1:30 (Tables 2 and 3). DOPC vesicles prior to irradiation were still quite leaky and the rates for ion permeation were ca. two fold higher compared with **1** and **2** at mole ratios of 1:20. Yet, following UV irradiation changes in the rates or extents of ion permeation were relatively similar to **1** and **2**. In lecithin vesicles, the rates of ion permeation for **15** and **16** were two fold lower than the controls and at least three fold lower than **1** and **2** prior to irradiation. However, lecithin vesicles including **16** were notably permeable whereas leakage from vesicles incorporating **15** was significantly reduced. This suggests that the dodecyl derivative is less disruptive and better organized within the lecithin vesicle membrane than the hexyl analog. Upon UV irradiation, the rates of ion permeation for **15** and **16** decreased by at least two fold, while the extents of ion permeation only decreased slightly as observed for **1** and **2**. In diPhyPC, nonirradiated vesicles at a 1:20 mole ratio were also more permeable in the presence of **15** and **16**. While in DPPC, the changes in the rates and extents of ion permeation were similar to **1** and **2**. From these studies, it is clear that the lack of a quaternary ammonium cation has a large effect on the ion permeabilities of fluid-phase lipid vesicles and relatively no effect in DPPC vesicles. These results suggest that the moderate increase in hydrophobicity of the ionizable derivatives reduces the overall lipid order within the membrane of fluid-phase lipid vesicles to a greater extent than DTEs with a cationic substituent. To further evaluate the effect

of DTE hydrophobicity on the stability of fluid-phase vesicles, asymmetrical DTE derivatives like **15** and **16** without terminal amino substituents will need to be prepared and examined.

Given DTEs are thermally stable in either isomeric state, we also examined the cycloreversion of **3** in DPPC at a mole ratio of 1:20 by preparing vesicles incorporated with closed-ring isomers and then irradiating these vesicles with visible light. Prior to visible irradiation, the rate constant of ion permeation for DPPC vesicles incorporating the closed-ring isomers of **3** was ca. three fold lower when compared with vesicles incorporating the open-ring isomers (i.e., $k = 0.97 \pm 0.04 \times 10^{-4}$ $s^{-1}$ and ratio = 2.1 vs. $k = 2.6 \pm 0.4 \times 10^{-4}$ $s^{-1}$ and ratio = 5.7, respectively). This was expected given the closed-ring isomers were found to be less disruptive in our UV irradiation studies. Upon visible irradiation, we observed a 50% increase in the ratio of rate constants (i.e., 2.1 to 3.1), which again we would anticipate given the open-ring isomers were found to be more disruptive. As a proof of concept, this result suggests that ion permeability can be reversibly controlled with light. However, further study is required as the current assay is not well suited for monitoring ion permeability as the DTE isomers are cycled with light because a base pulse is required to establish the transmembrane pH gradient for each measurement. We are currently developing an improved method to monitor changes in ion permeability as DTEs are cycled between the photoisomers.

## Conclusions

We have developed a synthetic method for amphiphilic DTEs that integrate a terminally charged alkyl chain, and contain methyl or phenylethynyl substituents at the reactive carbons. Our photochromic reactivity studies suggest that the inclusion of a single alkyl chain leads to a significant improvement in the cyclization quantum yield. Our ion permeation studies show that

the open-ring isomers of these DTEs are more disruptive (as monomers) than the closed-ring isomers in the four lipid vesicle systems studied, regardless of their lamellar phase. Still, ion permeation and the stability of the host vesicle are clearly sensitive to substituent effects. A preliminary investigation suggests that ion permeability can be reversibly controlled with light. However, a more thorough examination will be reported separately using a new analytical method and analogous DTEs with improved photostability. Overall, we have shown that asymmetrical amphiphilic dithienylethenes can be used as photoswitches to control ion permeation in lipid vesicles.

## Experimental

Synthetic procedures, including NMR and high-resolution mass spectra, are described in the electronic supplementary information (ESI).

**Instrumentation.** $^{1}$H, $^{19}$F, and $^{13}$C NMR spectra were recorded at 300.18, 282.46, and 75.48 MHz, respectively, on a Varian Mercury plus spectrometer (Palo Alto, CA, USA). Chemical shifts are referenced to solvent signals. $^{19}$F NMR spectra were recorded without $^{1}$H decoupling. $^{13}$C NMR spectra were recorded with $^{1}$H decoupling. High-resolution mass spectral analyses were carried out by the University of Calgary or University of Saskatchewan on a VG 70SE mass spectrometer (Manchester, UK) or API Qstar XL mass spectrometer (Carlsbad, US), respectively, which was operated in electrospray ionization mode, electron impact mode, or field desorption mode. HPLC analyses were performed on a HP 1090 Series II liquid chromatograph (Santa Clara, CA, USA). A guard column containing SecurityGuard ULTRA pentafluorophenyl (PFP) cartridges was connected to a Kinetex 2.6 μm PFP analytical column (150 mm × 4.6 mm

i.d.) from Phenomenex (Torrance, CA, USA). A gradient elution was run for **1** and **2** in which the mobile phase was initially 10:90 water/acetonitrile with each solvent containing 0.1% trifluoroacetic acid, and was gradually changed to 100% acetonitrile at 10 min. The flow rate was 1.2 mL $min^{-1}$, the injection volume was 5 μL, and signals were monitored at isosbestic points. An isocratic elution was run for **3** in which the flow rate was 1.4 mL $min^{-1}$ and the mobile phase was 8:92 water/methanol with each solvent containing 0.1% trifluoroacetic acid. Steady-state absorption spectra were obtained at constant temperature (e.g., 21.0 ± 0.1 °C) on a Cary 300 Bio UV–Vis spectrophotometer (Mississauga, ON, Canada) equipped with a dual cell Peltier circulator accessory. The absorption spectra were recorded at a scan rate, step size, and integration time of 300 nm $min^{-1}$, 0.5 nm, and 0.1 s, respectively. Steady-state fluorescence spectra were obtained at constant temperature (e.g., 21.0 ± 0.5 °C) with a PTI QuantaMaster spectrofluorometer (Birmingham, NJ, USA), and the excitation and emission slits were set such that the bandwidths were 2 nm. Excitation ratio experiments using HPTS were performed with excitation wavelengths of 403 and 460 nm and an emission wavelength of 510 nm. The integration time was 2 sec. For quantum yield studies and the HPTS assay, all samples were irradiated with a 300 W xenon light source from Luzchem (Ottawa, ON, Canada), measured in a 10 mm × 10 mm quartz Suprasil fluorescence cell from Hellma (Concord, ON, Canada) and stirred. For ultraviolet irradiations, the xenon light source was filtered with a bandpass filter (Hoya U-340, $\lambda_c$ = 340 ± 42 nm) and an aqueous solution of potassium chromate ($\lambda_c$ = 313 ± 7 nm[47] circulated through a 50 mm × 22 mm cylindrical cell from Hellma ($A_{313}$ = 0.040 ± 0.005). For visible irradiations, a bandpass filter (Thorlabs FB530-10, $\lambda_c$ = 530 ± 5 nm) was used. For photoconversion and photostability studies, ultraviolet irradiations of all samples were performed with a 6 W UVA ($\lambda_c$ = 365 nm) UltraLum TLC lamp. Visible irradiations in the photostability

studies were carried out with a 300 W Osram EXR halogen lamp of a Kodak Ektagraphic III E Plus slide projector fitted with a longpass filter (Schott GG-495, $\lambda_c = 495 \pm 6$ nm).

**Materials.** All reactants (99+%, Sigma-Aldrich, Oakville, ON, Canada), deuterated solvents (99.9 atom % D, Sigma-Aldrich), palladium catalysts (99.9+% Pd, Strem Chemicals, Newburyport, MA, USA), octafluorocyclopentene (OFCP; 99+%, SynQuest Laboratories, Alachua, FL, USA), lecithin (refined, Alfa Aesar, Ward Hill, MA, USA), Triton X-100 (scintillation grade, Eastman Kodak Company, Rochester, NY, USA), buffer salts (99+%, Sigma-Aldrich and Alfa Aesar), 1,2-dioleoyl-*sn*-glycero-3-phosphocholine (DOPC; >99%, Avanti Polar Lipids, Alabaster, AL, USA), 1,2-dipalmitoyl-*sn*-glycero-3-phosphocholine (DPPC; >99%, Avanti Polar Lipids) and 1,2-diphytanoyl-*sn*-glycero-3-phosphocholine (diPhyPC; >99%, Avanti Polar Lipids) were purchased and used as received. Carbon tetrachloride, copper (I) iodide, diethyl ether, 1,4-dioxane, THF and triethylamine were purified following literature procedures.[48] Flash column chromatography was performed on silica gel (230-400 mesh, 60 Å, Sillicycle, Quebec City, QC, Canada). 8-Hydroxypyrene-1,3,6-trisulfonic acid trisodium salt (HPTS; dye content ca. 75%, Sigma-Aldrich) was recrystallized from ethanol five times. Deionized water was obtained from a Milli-Q Gradient A10 water system (Millipore Corp., Mississauga, ON, Canada). All aqueous solutions were prepared in phosphate buffer (10 mM $Na_3PO_4$, 100 mM NaCl, pH adjusted to 6.4 using $H_3PO_4$).

**Quantum yield, photoconversion and photostability studies.** The cyclization and cycloreversion quantum yields of **1**–**3** in ethyl acetate were determined using Aberchrome 540 (A540) as a chemical actinometer. The procedures used to determine the quantum yields of

DTEs have been previously described in detail.[23] Briefly, the absorbance of the solution containing A540 was matched to a solution containing the DTE (i.e., **1**–**3**). The absorbances were matched at 313 nm and 530 nm for the cyclization and cycloreversion quantum yields, respectively. The matched solutions were irradiated with either UV or visible light for a known period of time under identical experimental conditions. After irradiation, the absorbance of each solution was measured immediately. To determine the cyclization quantum yield, the change in absorbance for the DTE solution before and after irradiation with UV light was measured at the $\lambda_{max}$ in the visible region. From the change in absorbance, the $\phi$ was calculated using Eq. 1,

$$\phi = \left[\frac{\log T_0}{(1-T_0)} - \frac{\log T_t}{(1-T_t)}\right] \times \frac{VN_A}{(h\nu/t) \times \varepsilon_{max} \times l \times t} \quad (1)$$

where $T_0$ is the transmittance ($T = 10^{-A}$) at the wavelength of maximum absorption ($\lambda_{max}$) before irradiation, $T_t$ is the transmittance at $\lambda_{max}$ after irradiation, $V$ is the irradiated volume (L), $N_A$ is the Avogadro constant, $h\nu/t$ is the photon rate determined from A540 in ethyl acetate[49], $\varepsilon_{max}$ is the molar absorptivity at $\lambda_{max}$, $l$ is the optical path length of the quartz cell, and $t$ is the irradiation time. The cycloreversion quantum yield was determined in a similar manner. Before the solutions containing A540 and the DTE were matched, they were irradiated with UV light for 15–20 min to their photostationary state. The absorbance of each solution was measured following irradiation with visible light. Given that the cycloreversion quantum yield of A540 in ethyl acetate at 530 nm has not been reported, the quantum yield of A540 in *n*-hexane[49] was used as a primary standard. The cycloreversion quantum yield of A540 in ethyl acetate was determined to be 0.032 ± 0.004.

The photoconversion from the open-ring to the closed-ring isomers in the photostationary state under irradiation with UV light was determined for **1**–**3** from HPLC studies. The integrated

area for the peak representing the closed-ring isomer was divided by the sum of the integrated areas for the peaks representing both isomers and was calculated as a percentage.

The photostability of **1**–**3** in ethyl acetate (0.07 μM) was measured by UV-vis absorption spectroscopy over five ring-closing/ring-opening cycles in the presence of air. For each DTE, the absorbance was monitored at the $\lambda_{max}$ for the ring-closed isomer upon reaching the photostationary state or complete cycloreversion. For **1** and **2**, 3 min of UV and 2 min of visible light were used in each cycle, whereas for **3**, 10 min of UV and 3 min of visible light were used in each cycle.

**Procedure for lipid vesicle preparation.** Similar procedures used to prepare lipid vesicles have been previously described in detail.[21] Briefly, lipid stock solutions (2 mg/mL) of DOPC, DPPC, diPhyPC, and lecithin were prepared in chloroform. Separate stock solutions of **1**–**3** in $CHCl_3$ (1 mM), and 8-hydroxypyrene-1,3,6-trisulfonic acid trisodium salt (HPTS; 10 μM) in phosphate buffer were prepared. The same procedure was used to prepare all lipid vesicles. For example, to prepare DOPC vesicles containing **1** at a mole ratio of 1:20 (**1**/DOPC), a stock solution of **1** (127 μL) and DOPC (1 mL) were added to a 10 mL round bottom flask. The $CHCl_3$ was evaporated under reduced pressure to deposit a lipid film. The lipid film was dried under vacuum for at least 3 h and then hydrated with HPTS (1 mL) at 50.0 ± 0.1 °C for a minimum of 3 h. The lipid suspension was left to stand overnight at 4 °C. The hydrated lipid suspension underwent 5 freeze and thaw cycles by placing the sample in a dry ice/acetone bath, followed by a warm water bath and vortexed for 30 s. The sample was extruded 21 times at constant temperature (50.0 ± 0.5 °C) using 0.1 μm polycarbonate membrane filters. The sample was loaded onto a buffered PD MidiTrap G-25 desalting column and eluted with 1.5 mL of buffer to

remove extravesicular HPTS. The first 5 drops of eluent were discarded to give a purified lipid vesicle sample (ca. 1.3 mg/mL).

**HPTS ion transport assay.** The protocol for the HPTS fluorescence assay has been adapted from a previously published procedure.[37] Briefly, 2 mL of phosphate buffer and 100 μL of the lipid vesicle sample were added to a fluorescence cell and stirred. For nonirradiated samples, 50 μL of 0.5 M NaOH was added following a 150 s equilibration period. After 700 s, the vesicles were lysed with 50 μL of a 5% Triton X-100 solution. For irradiated samples, the base was added following a 70 s equilibration period, which was preceded by 3 min of UV irradiation, and an initial 80 s equilibration period. All data during the 150 s equilibration period and ca. 30 s after the addition of base was ignored when fitting the data (i.e., ca. 180 s was $t_0$). The relative emission intensity $E_{403}/E_{460}$ ($I$) was calculated. The extent of ion permeation ($N_t$) was calculated using Eq. 2,

$$N_t = \frac{(I_t - I_0)}{(I_\infty - I_0)} \qquad (2)$$

where $I_t$ is the relative emission intensity at time $t$, $I_0$ is the relative emission intensity at $t_0$, and $I_\infty$ is the relative emission intensity when the vesicles are lysed. The extent of ion diffusion was plotted against time, and the slope from the linear fit represents the rate constant for ion permeation. Upon irradiation of vesicles incorporating DTEs some quenching of the HPTS emission was observed because the closed-ring isomers do have weak absorption at 510 nm. This emission quenching correlated well with DTE photoconversion and resulted in an apparent increase in the extent of ion permeation before the addition of base. In these cases, the extent of ion permeation prior to lysis was corrected by subtraction of this experimental artifact.

To assess aggregation behavior, the extent of ion permeation at 700 s ($N_{700}$) for the various mole ratios of DTE in DPPC vesicles was used. The mole ratios that gave the minimal and maximal extent of ion permeation (i.e., $N_{MIN}$ and $N_{MAX}$) were used to recalibrate for a fractional activity ($Y$) using Eq. 3,

$$Y = \frac{(N_{700} - N_{MIN})}{(N_{MAX} - N_{MIN})} \quad (3)$$

A plot of $Y$ as a function of the concentration of DTE yielded a sigmoidal curve. The Hill coefficient $n$ was obtained from the curve fit using the Hill equation (Eq. 4)[50],

$$Y = Y_\infty + (Y_0 - Y_\infty) / (1 + (c / K_D)^n) \quad (4)$$

where $Y_0$ is $Y$ in the absence of DTE, $Y_\infty$ is $Y$ in the presence of excess, $c$ is the DTE concentration and $K_D$ is the dissociation constant.

**Acknowledgments**

We would like to express our gratitude to the Natural Sciences and Engineering Research Council (NSERC) of Canada and the University of Regina for support of this work.

**Bibliographic references**

1. W. A. Velema, W. Szymanski and B. L. Feringa, *J. Am. Chem. Soc.*, 2014, **136**, 2178-2191.
2. N. Fomina, J. Sankaranarayanan and A. Almutairi, *Adv. Drug Deliv. Rev.*, 2012, **64**, 1005-1020.
3. A. Yavlovich, B. Smith, K. Gupta, R. Blumenthal and A. Puri, *Mol. Membr. Biol.*, 2010, **27**, 364-381.

4. J. Y. Wang, Q. F. Wu, J. P. Li, Q. S. Ren, Y. L. Wang and X. M. Liu, *Mini Rev. Med. Chem.*, 2010, **10**, 172-181.
5. F. Ercole, T. P. Davis and R. A. Evans, *Polym. Chem.*, 2010, **1**, 37-54.
6. C. Alvarez-Lorenzo, L. Bromberg and A. Concheiro, *Photochem. Photobiol.*, 2009, **85**, 848-860.
7. P. Shum, J.-M. Kim and D. H. Thompson, *Adv. Drug Delivery Rev.*, 2001, **53**, 273-284.
8. B. Bondurant, A. Mueller and D. F. O'Brien, *Biochim. Biophys. Acta*, 2001, **1511**, 113-122.
9. B. Chandra, R. Subramaniam, S. Mallik and D. K. Srivastava, *Org. Biomol. Chem.*, 2006, **4**, 1730-1740.
10. Y. Y. Lin, X. H. Cheng, Y. Qiao, C. L. Yu, Z. B. Li, Y. Yan and J. B. Huang, *Soft Matter*, 2010, **6**, 902-908.
11. R. M. Uda, E. Hiraishi, R. Ohnishi, Y. Nakahara and K. Kimura, *Langmuir*, 2010, **26**, 5444-5450.
12. A. Yavlovich, A. Singh, R. Blumenthal and A. Puri, *Biochim. Biophys. Acta, Biomembr.*, 2011, **1808**, 117-126.
13. Y. Lei and J. K. Hurst, *Langmuir*, 1999, **15**, 3424-3429.
14. R. F. Khairutdinov and J. K. Hurst, *Langmuir*, 2001, **17**, 6881-6886.
15. M. Irie, *Chem. Rev.*, 2000, **100**, 1685-1716.
16. T. Hirose, K. Matsuda and M. Irie, *J. Org. Chem.*, 2006, **71**, 7499-7508.
17. Y. Zou, T. Yi, S. Z. Xiao, F. Y. Li, C. Y. Li, X. Gao, J. C. Wu, M. X. Yu and C. H. Huang, *J. Am. Chem. Soc.*, 2008, **130**, 15750-15751.
18. X. Zhou, Y. Duan, S. Yan, Z. Liu, C. Zhang, L. Yao and G. Cui, *Chem. Commun.*, 2011, **47**, 6876-6878.

19. S. M. Polyakova, V. N. Belov, M. L. Bossi and S. W. Hell, *Eur. J. Org. Chem.*, 2011, 3301-3312.

20. J. T. van Herpt, J. Areephong, M. C. A. Stuart, W. R. Browne and B. L. Feringa, *Chem.–Eur. J.*, 2014, **20**, 1737-1742.

21. Y. Bai, K. M. Louis and R. S. Murphy, *J. Photochem. Photobiol., A*, 2007, **192**, 130-141.

22. K. Morimitsu, S. Kobatake and M. Irie, *Tetrahedron Lett.*, 2004, **45**, 1155-1158.

23. J. X. Cai, A. Farhat, P. B. Tsitovitch, V. Bodani, R. D. Toogood and R. S. Murphy, *J. Photochem. Photobiol., A*, 2010, **212**, 176-182.

24. L. Aurelio, R. T. C. Brownlee and A. B. Hughes, *Chem. Rev.*, 2004, **104**, 5823-5846.

25. R. E. Bowman and H. H. Stroud, *J. Chem. Soc.*, 1950, 1342-1345.

26. J. Cheung, L. D. Field and S. Sternhell, *J. Org. Chem.*, 1997, **62**, 7044-7046.

27. S. Ito, M. Wehmeier, J. D. Brand, C. Kubel, R. Epsch, J. P. Rabe and K. Mullen, *Chem.–Eur. J.*, 2000, **6**, 4327-4342.

28. V. A. Smirnov and A. E. Lipkin, *Khim. Geterotsikl. Soedin.*, 1973, 185-187.

29. Y. Goldberg and H. Alper, *J. Org. Chem.*, 1993, **58**, 3072-3075.

30. M. Irie, T. Lifka, S. Kobatake and N. Kato, *J. Am. Chem. Soc.*, 2000, **122**, 4871-4876.

31. M. Irie, T. Lifka, K. Uchida, S. Kobatake and Y. Shindo, *Chem. Commun.*, 1999, 747-748.

32. A. Peters and N. R. Branda, *Adv. Mater. Opt. Electron.*, 2000, **10**, 245-249.

33. P. D. Patel, I. A. Mikhailov, K. D. Belfield and A. E. Masunov, *Int. J. Quantum Chem.*, 2009, **109**, 3711-3722.

34. E. C. Harvey, J. Areephong, A. A. Cafolla, C. Long, W. R. Browne, B. L. Feringa and M. T. Pryce, *Organometallics*, 2014, **33**, 447-456.

35. P. Celani, S. Ottani, M. Olivucci, F. Bernardi and M. A. Robb, *J. Am. Chem. Soc.*, 1994, **116**, 10141-10151.

36. K. Higashiguchi, K. Matsuda, S. Kobatake, T. Yamada, T. Kawai and M. Irie, *Bull. Chem. Soc. Jpn.*, 2000, **73**, 2389-2394.

37. T. M. Fyles and H. Luong, *Org. Biomol. Chem.*, 2009, **7**, 733-738.

38. S. Matile and N. Sakai, in *Analytical Methods in Supramolecular Chemistry*, ed. C. Schalley, Wiley-VCH, Weinheim, 1st edn., 2007, pp. 391-418.

39. D. Marsh, *Handbook of Lipid Bilayers*, CRC Press, Boca Raton, 2nd edn., 2013.

40. H. Lindsey, N. O. Petersen and S. I. Chan, *Biochim. Biophys. Acta*, 1979, **555**, 147-167.

41. D. D. Lasic, *Liposomes: From Physics to Applications*, Elsevier Science, New York, 1993.

42. S. Paula, A. G. Volkov, A. N. VanHoek, T. H. Haines and D. W. Deamer, *Biophys. J.*, 1996, **70**, 339-348.

43. X. D. Song, J. Perlstein and D. G. Whitten, *J. Am. Chem. Soc.*, 1997, **119**, 9144-9159.

44. J. M. Moszynski and T. M. Fyles, *Org. Biomol. Chem.*, 2010, **8**, 5139-5149.

45. C. J. Wohl, M. A. Helms, J. O. Chung and D. Kuciauskas, *J. Phys. Chem. B*, 2006, **110**, 22796-22803.

46. A. Hennig, L. Fischer, G. Guichard and S. Matile, *J. Am. Chem. Soc.*, 2009, **131**, 16889-16895.

47. J. G. Calvert and J. N. Pitts, Jr., *Photochemistry*, Wiley & Sons, New York, 1966.

48. D. D. Perrin and W. L. Armarego, *Purification of Laboratory Chemicals*, Elsevier Science, New York, 3rd edn., 1988.

49. H. G. Heller and J. R. Langan, *J. Chem. Soc., Perkin Trans. 2*, 1981, 341-343.

50. S. Litvinchuk, G. Bollot, J. Mareda, A. Som, D. Ronan, M. R. Shah, P. Perrottet, N. Sakai and S. Matile, *J. Am. Chem. Soc.*, 2004, **126**, 10067-10075.